Title: Multi-axial mechanical characterization of jute fiber/polyester composite materials

Authors: **Yousef Dobah** [a]

Mostefa Bourchak [b]

Abderrezak Bezazi [c]

Ahmed Belaadi [c,d]

Fabrizio Scarpa [e]

[a] Mechanical Engineering Department, University of Jeddah, Jeddah, Saudi Arabia

Email: ydobah@uj.edu.sa Telephone: +966126400000 Ext.: 74086

[b] Aeronautical Engineering Department, King Abdulaziz University, Jeddah, Saudi Arabia

Email: mbourchak@kau.edu.sa

[c] Laboratoire de Mécanique Appliquée des Nouveaux Matériaux (LMANM), B.P. 401, Université 8 Mai 1945 Guelma, Algeria.

Email: ar_bezazi@yahoo.com ahmedbelaadi1@yahoo.fr

[d] Université 20 août 1955 - Skikda, B.P.26 route El-Hadaiek, 21000 Skikda-Algeria.

Email: ahmedbelaadi1@yahoo.fr

[e] Corresponding Author: Advanced Composites Centre for Innovation and Science (ACCIS) University of Bristol, UK; Bristol Centre for Nanoscience and Quantum Information (NSQI) University of Bristol, UK

Email: f.scarpa@bristol.ac.uk

ABSTRACT

The work describes the mechanics of novel woven jute fibers reinforced polyester (JFRP) laminates under uniaxial and multi-axial static and fatigue loading cases. JFRP laminates with 25 % fibre volume fraction (FVF) have been manufactured using a hand-layup molding technique at a low pressure. Static uniaxial tests have shown that these novel bio-reinforced laminates have an ultimate tensile strength around 42 MPa under tensile loading and 7.5 N-m under torsional loading. The Multi-axial (tension/torsion) static tests yield an ultimate strength of 21.7 MPa and 5 N-m for tensile and torsion loading conditions, respectively. Fatigue tests have been carried out under displacement and angular control at three different loading levels with a frequency of 5Hz. The fatigue tests results are extensively analyzed using stiffness degradation behavior, hysteresis loops, energy dissipation and strain versus number of cycles (ε-N) diagrams. The fatigue endurance limit (over one million cycles) for JFRP is achieved at a stress level of 65% of ultimate displacement. The implication of this work is the use of these materials in areas such as car and aircraft interiors promises to significantly reduce weight, cost and carbon footprints without sacrificing performance.

Keywords: Polymer-matrix composites (PMCs); Fatigue; Mechanical Testing; Lay-up (manual); Natural Fibers

1 INTRODUCTION

Companies and researchers are driven by current environmental requirements to develop new materials that can replace synthetic fibers (e.g. glass fibers) with enhanced life cycle performance. Natural fibers as reinforcement in composite materials show some appealing characteristics like low cost, low density, relativly high specific strength and ease of availability where they are readily available in fibrous form [1]. The dependency on fossil fuel products and their environmental hazards would eventually be minimized by the use of such fibers to produce bio-composite materials and products. Engineers have already succeeded to implement natural fibers in the production of bio-composite materials that are suitable for secondary structural applications on an industrial scale [2]. Many researchers have performed the mechanical characterization of different types of natural fibers and their composites [3–6]. Some works in open literature show comparative studies to identify which natural fiber have superior mechanical properties [7]. Other studies provide expanded databases of experimental results related to particular types of natural fibers [8–12]. Some research groups have also attempted to find how different factors affect the performance of existing natural fibers composites [13–17]. Jute fibers are typical examples of natural fibrous reinforcement extracted from the stem of Jute plants, and are one of the most affordable natural fibers available in the market, second only to cotton in terms of amount produced and varieties of applications (baskets, carpets, shoes, cloths and ropes). Several research groups have carried extensive studies on the mechanical properties of jute fibers and its derived plastic composites [18–25]. Katogi et al [21] tested unidirectional jute spun yarn reinforced biodegradable resin under static and fatigue tensile loading. They reported an ultimate tensile strength of 60.9 MPa and an endurance limit of 55% for their composite material. Gassan [22] has investigated the effect of fibers type, fibers treatment, fibers form, fiber content and matrix type on the material's specific damping capacity under tension-tension fatigue loading tests. Regarding jute fabric reinforced polyester composites; he found treating the jute surface with silane will require higher loads for the onset of progressive damage. Gowda et al [23] have evaluated the mechanical properties of untreated jute fibers and fabrics, and jute fabric reinforced composites under static loading. Single jute fibers exhibited stiffer mechanical behavior than jute fabrics. Shah et al [24] have also

investigated the effect of fibers type, content, form and stress ratio on the tension-tension fatigue life of natural fibers composites, comparing unidirectional jute yarns reinforced polyesters to hemp and flax yarns reinforced polyesters. The jute fibers composites showed one of the highest tensile static and fatigue strength compared with other natural composites, second only to flax composites. The **jute** composite material did also survive million of cycles under fatigue loading at a stress ratio of 45%. Shah and co-workers also found that higher jute fiber contents would increase the static and fatigue strength of the overall composites. The increased fibers content did also influence the mechanism associated to the specimen failure, ranging from stable transverse cracks in the matrix to the presence of jagged, delaminated and longitudinal splitting cracks. De Rosa et al [25] have looked at the production of recycled secondary structural composites made from **paper** waste, jute fabric and epoxy matrix, and performed extensive static and acoustic emissions (AE) tests under flexural bending on these samples. The tests showed that the use of waste **paper** increased significantly the flexural modulus of the natural reinforced composites, while the AE analysis gave some significant insight on the role of the stacking sequence and phase materials used.

Multi-axial testing has attracted many researchers [26] by several reasons. For example, many component in service are actually under combind loadings which is represnted better by the multi-axial loading tests. It is a huge study field that still lack testing standards and databases. M. Quaresimin et al [27] reviewed the work done on multi-axial fatigue testing of composite materials and highlighted a significant effect of the shear stress on the fatigue life of a component. Also, they point out the scarce data of a rectangular sample under multi-axial loading due to the fact of the non-uniform stress distribution on the cross section of the sample. Amijima et al [28] represented the data of multi-axial tension-torsion fatigue tests as the ratio between each loading type results by its pure application results, then combined the different ratios to represent the results of multi-axial loading. They deducted that the fatigue life depends on the loading ratio between the two loading types used in the multi-axial tests. Ogasawara et al [29] performed another type of multi-axial testing where they applied a fixed tensile loading and cycled the torsional loading at the same time. They eliminated the need to represent the results as variable of both tensile and torsional loadings. The study shows that the tensile load level has a positive impact on the torsional rigidity of any sample.

The current study is focused on the mechanics of untreated woven jute fabric used to reinforce polyester matrix systems under tensile, torsional and multi-axial static and fatigue loading conditions. Fatigue tests are carried out under variable amplitude tensile (tension-tension) and multi-axial (tension-tension - unidirectional torsion) loading conditions. Stiffness degradation is monitored during fatigue tests and ε-N curves are constructed to reflect the fatigue damage inflicted on the specimens. Hysteresis loops are also constructed and the energy dissipation is calculated to determine the amount of damage that was accumulated at various load levels. To the best of the Author's knowledge, this is the first study in which multi-axial fatigue tests are performed on jute/polyester composites.

2 MATERIAL PREPARATION, TEST SETUP AND DATA REPRESENTATION

The jute fabric used in this study was bought from a local supplier and used as received. The polyester used to fabricate the composites has a 32 MPa in tensile strength, 2.7 % in elongation, 1.12 GPa in tensile modulus, and a density of 1410 kg/m^3. The jute fibers reinforced polyester (JFRP) laminates were manufactured at low pressure using a hand-layup composites fabrication technique inside a glass mold with glass shims to control laminate thickness at room temperature. The laminates were made by cutting the jute fabric into three plies, and then adding polyester resin to each one of them. Afterwards, the plies were carefully stacked on top of each other inside the mold. The plates were allowed to cure for 24 hours at room temperature inside the mold. The plates were kept in open air for 15 days to obtain a complete polymerization of the resin,. The specimens were then cut from the plates using a diamond saw, following the recommendations of the ASTM Standard D 3039 M-08. The dimensions of the manufactured plates are 320 x 380 x 5 mm, while each single **composite** specimen has dimensions of 250 x 25 x 5 mm. It is worth to notice that, although these dimensions are standard for tensile tests, similar specimen sizes were used in a previous work by H.T.Sumsion et al [30] to perform torsional loading experiments.

The mechanical tests were carried out using a MTS 809 Axial Torsional Testing System with a load cell capacity of 100 (± 0.1) kN in tension and 1100 (± 1.1) N-m for torsion. Tensile static tests were performed at a constant rate of 5 mm/min, while torsional static tests were carried out at 30 degree/min. The multi-axial static tests were performed at a combined rate of 2 mm/min and 83 degree/min;

corresponding to the time required to fail a specimen under either tensile or torsion loads. The resulted biaxiality ratio is 1.27, which is defined as the ratio of torsional property to tensile property; the property is defined as ratio of ultimate multi-axial strength to ultimate uniaxial strength[31]. Tensile and multi-axial fatigue tests were performed under displacement and angular control with a sinusoidal waveform of 5 Hz. All fatigue tests were carried out at a mean strain level corresponding to 50 % of the ultimate tensile or torsional strains. The straining level (r) was defined as a percentage from the average failure strain identified from the respective static tests. The straining levels used in these tests were at 65%, 70% and 75%. These values were chosen based on some preliminary tests results. The fatigue test has been repeated at least twice for each value of (r). The tests were performed at room temperature (around 23°C) and average humidity of 50 %.

The results of the multi-axial fatigue testing are represented by combining both the data from the two types of loading (tensile and torsional). The stiffness degradation is found by averaging the normalized stiffness loss from both loading types. The hysteresis loops represent the averaged normalized loading from both types of loop data. Finally, the dissipated energy is represented be the total energy lost by the longitudinal and lateral movements of the sample. The resulted data from this method is compared to the results from the static-to-fatigue ratio method proposed by Amijima et al [28].

3 RESULTS AND DISCUSSIONS

3.1 Static Results

3.1.1 Tensile static test

Fig.1 shows the stress and strain curves of three tested JFRP specimens, while Table 1 illustrates the values of stresses and strains corresponding to failure and their averaged values. All specimens show a similar mechanical behavior, with the stiffness slightly decreasing beyond 0.1% elongation and a complete failure occurring around 1.1% elongation. Multiple fluctuations were observed before the complete failure of the specimens, which indicate partial fibers failure and can be caused by the presence of random voids

into the matrix. The uncovered **areas of the specimens** along the length of the fibers form stress concentration points, which develop very fast crack propagation when the fibers fail. It has also been noticed that the weave-fabricated fibers are not uniform in term of distribution of fibers threads diameters and spaces between them. An example of the topology of the fabrics can be observed in Fig.2, which shows that the crack in the composite followed a straight line through the material with some fibers being pulled out from the matrix, although the weave topology of the fabric helped to reduce the number of pullouts.

3.1.2 Torsional static tests

Fig.3 shows torque versus the angular displacement in JFRP specimens. Table.2 shows the ultimate torque strengths and angular displacements at failure values. Cracks started appearing on the specimens at around 55 degrees but the specimens continued carrying the load until a complete failure occurred between 70 and 80 degrees. Due to the geometry of the specimens, the angular displacement at failure must be considered significant, demonstrating that these composites offer a significant compliance in terms of torsional deformation. One reason of this specimen high torsional compliance is the use of a thermoset matrix system that has a relatively high elongation percentage. The failure surface of a JFRP specimen under static torsional load can be observed in Fig. 4. The cracks start from the two edges of the specimens forming a Z-shaped cut. The morphology of the cut indicates that high shearing stresses are present between the composites layers undergoing delamination. These shear stresses make the fibers at the edge to carry alone the tensile loading and therefore fail first. After that initial failure the load is transferred from one layer to the other, creating the unique shape of the cut.

3.1.3 Multi-axial static tests

Figs. 5 (a) and (b) show the behavior of the composite material corresponding to the multi-axial load configuration used. Figure 5(a) shows the stress vs. strain relation due to tensile load, while Figure 5(b) illustrates the torque vs. the angle. The tensile and torque loading were applied simultaneously as observed from the curves, which show the same overall mechanical behavior consisting in a progressive decrease of

stiffness and the occurrence of partial fibers breaking until reaching a complete failure. Fig.6 shows the shape of the fracture section of a JFRP specimen under the static multi-axial loading. The Z-shape cut produced from applying the torsional load observed earlier provides a less evident shear band because of the application of the simultaneous tensile load. Table.3 shows the failure values of stresses for the multi-axial loading. It is apparent that the application of a simultaneous tension and torsional load specimens with the chosen loading rates reduced its ultimate tensile strength by 49% and its ultimate torque strength by 35%, simultaneously. It is hard to compare this finding with other literature due to differences in the geometry of the samples, biaxiality ratio and the fibers direction and weaving properties of the composites laminates. For example, D. Qi and G. Cheng [31] reported higher reduction in the properties for a biaxiality ratio of 1 (52%, for tensile strength and 49% for torque strength). They used tubular samples with different filament winding degrees that effect greatly the reduction of the different properties.

3.2 Fatigue Results

3.2.1 STIFFNESS DEGRADATION

The identification of material's stiffness degradation is one of most used methods to evaluate the accumulated fatigue damage [11]. It is identified through tracking the change in the load experienced by a specimen under constant strain, which indicates the amount of material's stiffness degradation by each loading cycle. Fig.7 shows a typical load degradation behavior of JFRP composite with the number of cycles for both the tensile and the multi-axial fatigue tests. The curve of tensile fatigue stiffness degradation has been normalized by dividing the load (F) by maximum load recorded during the first cycle (F_0). The multi-axial fatigue stiffness degradation's curve has been constructed by combining the normalized stiffness degradation resulted from both tensile and torsional loads. The normalized number of cycles has been calculated by dividing the number of cycles (N) by the number of failure cycle (N_f). The JFRP specimen appears to follow the classic behavior in fatigue testing, which is made of three stages (rapid stiffness loss, followed by slow decrease in stiffness and finally, a complete failure at the end [32]). The matrix undergoes deformation and cracks start to propagate until the load is completely transferred to the

fibers (stage 1). The fibers begin to strain slowly making the cracks grow slower than before and gradually the matrix debonds from the fibers (stage 2). Finally, the fibers start to fail making fast cracks propagations that cause sudden global failure of the specimen (stage 3). It can be observed that the first stage lasted longer under normalized cycles for the case of the specimen undergoing multi-axial fatigue loading. This is believed to be originated from the combined crack propagation mechanism caused when applying tensile and torsional loads at the same time. Overall, the stiffness degradation appears to be more significant during the multi-axial loading case. On the other hand, the results of the multi-axial loading represented by the method suggested in this work shows almost identical values to Amijima et al [28] method that they use to represent the data of a similar loading case. The comparison of the two methods is shown in fig.8.

Fig.9 shows the tensile stiffness degradation (F/F_0) according to the number of cycles for different straining levels (r) using semi-logarithmic scale. The tensile fatigue life appears to depend upon the straining level (r). At r = 75%, the specimen failed after 16,000 cycles, but at smaller (r) values crack propagations are activated with a slow velocity and the fatigue life is remarkably longer. The total failure for the JFRP at straining level r = 70% happened after 80,000 cycles. However, at (r) = 65 % there is no global failure of the specimens even after 10^6 cycles, which is considered as the endurance limit under pure tensile loading condition. The composite is found to be losing 54% of its strength. For all the loading ratios used; the JFRP specimens appear to have the same stiffness degradation under 70 loading cycles.

Fig.10 shows the stiffness degradation resulting from the multi-axial fatigue tests. The same observations regarding the stiffness degradation behavior of the tensile fatigue tests can be also made for these curves, although the curves corresponding to 75% and 65% straining levels, results show a more gradual global failure compared to the one observed in the tensile loading case. The complete failure of the JFRP specimens under multi-axial loading happens after 90,000 cycles at (r) = 75%, and after 260,000 cycles at 70% of straining level. Also in this case, the endurance limit for the JFRP under multi-axial loads can be observed at 65% straining level for which the composite material losses 50% of its stiffness strength.

3.2.2 HYSTERESIS LOOPS AND DISSIPATED ENERGY DENSITY

The monitoring of the energy dissipation gives an indication about how fast the crack grows, and the idnetification of the hysteresis loops is the first step to perform this operation [12]. Hysteresis loops are shown in fig.11 for the first cycle at each different straining level for both tensile and multi-axial fatigue tests. To facilitate the comparison the loops have been normalized by dividing the cyclic load with the maximum load in each cycle. The hysteresis loops for multi-axial fatigue tests have also been calculated from the average of the normalized tensile and torsional loads values. For a clearer representation of the loops, the displacements of the cycles have been shifted by 0.5 mm each. The JFRP specimens contain some random voids with different sizes in the matrix that create onsets of crack propagation. As expected, a higher straining level will make the specimen to be subjected to broader spectrum of load amplitudes. The specimen deforms further, with a subsequent faster crack growth rate. The area inside the loop indicates how much energy is dissipated during the cycle, and it is proportional to the applied straining level [12].The energy density is larger during tensile fatigue tests, indicating that for each cycle the material tends to dissipate the majority of the energy under tensile deformation mechanisms (Figs. 12 and 13) .

The dissipated energy density [12] (or energy dissipation per unit volume) was measured for the two loading cases. In the case of the pure tensile loading (Fig.12), at 75% straining level the values of the dissipated energy density almost tripled compared to the values observed at (r) = 65%. All the curves can be divided into two stages. The first stage corresponds to a marked decrease of the energy dissipated per unit volume from the first cycle until 100 cycles for (r) = 75%, and 1000 cycles at (r) = 70% and 65%. The second stage is defined by a lower decreasing rate of the dissipated energy density until complete failure occurs at (r) = 75% and 70%. The 65% straining level curves show an almost steady decrease in the dissipated energy without failure, even after 10^6 cycles. The same observations can also be made about the total dissipated energy density of the multi-axial fatigue tests (Fig 13), although more fluctuations of the energy values could be observed for the multi-axial loading case. Note that the values represented in fig.13 are the sum of the dissipated energy density resulted from both tensile and torsional loadings.

3.2.3 r-N CURVE

The fatigue damage limit of a material can be determined by projecting the number of cycles to failure at different straining levels. Fig.14 shows the number of the cycles at failure for each straining level used in this work. The results have been fitted by a logarithmic equation that can be described by the simple relation [12]:

$$R = a - b \times \log N_R \qquad (1)$$

Straining level of 65% tests were stopped at different number of cycles exceeding the number of $1.35x10^6$, giving therefore the confidence that the endurance limit of the material was identified. Remarkably, this finding is true and the same for both pure tension and tension/torsion loading conditions. Note that the multi-axial fatigue loading case is incorporating approximately 36% of the material's ultimate tensile strength, which is way beyond the material's endurance limit for the tensile fatigue loading case. On other hand, although the test machine has a lower load sensitivity in the torsional channel (±1.1 N-m), the confidence in the projected multi-axial fatigue tests results is higher than the pure tensile fatigue tests results. It is thought as an indication of the complex failing mechanisms of the tension/torsion loading case that accumulate drastically at some point in the material's fatigue life.

4 CONCLUSIONS

Jute fiber reinforced polyester composite laminates were manufactured using a hand-layup low pressure molding technique. Specimens cut from these laminates were tested under tensile, torsional and multi-axial static loading. Also, specimens were tested under pure tensile and multi-axial fatigue loading. Static results showed small scatter in tensile data but wide scatter in torsional data. The results of multi-axial tests were affected by the fact that the specimen torsional strength was at the lower end of the machine capacity, which can go up to 1100 N-m. JFRP ultimate tensile strength was slightly lower than what have been found in earlier studies [23,24]. There is also a lack of tests' standards for composite materials under torsional load and multi-axial loads. Fatigue results were analyzed by monitoring the stiffness degradation, hysteresis loops and energy dissipation density (energy dissipation per unit volume).

The specimen stiffness degradation under constant amplitude fatigue loading was found to follow the common 3-stage fatigue life observed in many materials. The stages are rapid degradation stage, steady degradation stage and final failure stage. Hysteresis loops and energy dissipation for various load levels revealed a proportional behavior of number of cycles to straining level with the specimen achieving a fatigue strength level at about 65% (endurance limit). The latter level was higher than most recent study [24] and it was confirmed by both tensile and multi-axial fatigue loading tests results. **The tests results shown in this paper are indicative of very interesting mechanical properties under multi-axial loading that these natural fibre reinforced composites possess. The overall mechanical performance of these composites may be improved by using more advanced composites fabrication techniques like resin transfer molding, which tends to minimize the formation of matrix voids and to increase the compactness of the fibers. In addition, other types of fibers, fabric weaving and their chemical treatments are all factors that need to be taken into account in future investigation to widen the database of the results originated from using this testing method.**

5 REFERENCES

[1] Joshi S V., Drzal LT, Mohanty AK, Arora S. Are natural fiber composites environmentally superior to glass fiber reinforced composites? Compos Part A Appl Sci Manuf 2004;35:371–6. doi:10.1016/j.compositesa.2003.09.016.

[2] S.Das. Jute composite and its Applications. Int. Work. Jute Geotext., 2010.

[3] Jorge Parga Silva A, Antonio Rocco Lahr F, Luis Christoforo A, Hallak Panzera T. Properties of Sugar Cane Bagasse to Use in OSB. Int J Mater Eng 2012;2:50–6. doi:10.5923/j.ijme.20120204.04.

[4] Da Silva LJ, Panzera TH, Velloso VR, Christoforo AL, Scarpa F. Hybrid polymeric composites reinforced with sisal fibres and silica microparticles. Compos Part B Eng 2012;43:3436–44. doi:10.1016/j.compositesb.2012.01.026.

[5] Santulli C, Caruso AP. Effect of fibre architecture on the falling weight impact properties of hemp/epoxy composites. J Biobased Mater Bioenergy 2009;3:291–7. doi:10.1166/jbmb.2009.1037.

[6] De Vasconcellos DS, Sarasini F, Touchard F, Chocinski-Arnault L, Pucci M, Santulli C, et al. Influence of low velocity impact on fatigue behaviour of woven hemp fibre reinforced epoxy composites. Compos Part B Eng 2014;66:46–57. doi:10.1016/j.compositesb.2014.04.025.

[7] Ratna Prasad A V., Mohana Rao K. Mechanical properties of natural fibre reinforced polyester composites: Jowar, sisal and bamboo. Mater Des 2011;32:4658–63. doi:10.1016/j.matdes.2011.03.015.

[8] Bouakba M, Bezazi A, Boba K, Scarpa F, Bellamy S. Cactus fibre/polyester biocomposites: Manufacturing, quasi-static mechanical and fatigue characterisation. Compos Sci Technol 2013;74:150–9. doi:10.1016/j.compscitech.2012.10.009.

[9] Belaadi A, Bezazi A, Bourchak M, Scarpa F. Tensile static and fatigue behaviour of sisal fibres. Mater Des 2013;46:76–83. doi:10.1016/j.matdes.2012.09.048.

[10] Li Y, Mai Y-W, Ye L. Sisal fibre and its composites: a review of recent developments. Compos Sci Technol 2000;60:2037–55. doi:10.1016/S0266-3538(00)00101-9.

[11] Silva FDA, Chawla N, de Toledo Filho RD. An experimental investigation of the fatigue behavior of sisal fibers. Mater Sci Eng A 2009;516:90–5. doi:10.1016/j.msea.2009.03.026.

[12] Dobah Y, Bourchak M, Bezazi A, Belaadi A. Static and fatigue strength characterization of sisal fiber reinforced polyester composite material. Compos. Sci. Technol. 2020scientific Tech. challenges, 2013, p. 394–403.

[13] Towo AN, Ansell MP. Fatigue of sisal fibre reinforced composites: Constant-life diagrams and hysteresis loop capture. Compos Sci Technol 2008;68:915–24. doi:10.1016/j.compscitech.2007.08.021.

[14] Sangthong S, Pongprayoon T, Yanumet N. Mechanical property improvement of unsaturated polyester composite reinforced with admicellar-treated sisal fibers. Compos Part A Appl Sci Manuf 2009;40:687–94. doi:10.1016/j.compositesa.2008.12.004.

[15] Santos JKD, Cunha RAD, Felipe RCTS, Felipe RNB, Medeiros GG. Composite friend sisal / polyester treated in surface. HOLOS, Ano 27, Vol3 2011:102–11.

[16] Kim HJ, Seo DW. Effect of water absorption fatigue on mechanical properties of sisal textile-reinforced composites. Int J Fatigue 2006;28:1307–14. doi:10.1016/j.ijfatigue.2006.02.018.

[17] Basu G, Roy AN, Satapathy KK, Abbas SMJ, Mishra L, Chakraborty R. Potentiality for value-added technical use of Indian sisal. Ind Crops Prod 2012;36:33–40. doi:10.1016/j.indcrop.2011.08.001.

[18] Mishra V, Biswas S. Physical and mechanical properties of bi-directional jute fiber epoxy composites. Procedia Eng 2013;51:561–6. doi:10.1016/j.proeng.2013.01.079.

[19] Shaikh AA, Channiwala SA. Experimental and Analytical Investigation of Jute Polyester Composite for Long Continuous Fiber Reinforcement. J Reinf Plast Compos 2006;25:863–73. doi:10.1177/0731684406065138.

[20] Karaduman Y, Onal L. Dynamic mechanical and thermal properties of enzyme-treated jute/polyester composites. J Compos Mater 2012. doi:10.1177/0021998312457885.

[21] Katogi H, Shimamura Y, Tohgo T, Fujii T. Fatigue Behavior of Unidirectional Jute Spun Yarn. 18TH Int. Conf. Compos. Mater., 2011.

[22] Gassan J. A study of fibre and interface parameters affecting the fatigue behaviour of natural fibre composites. Compos - Part A Appl Sci Manuf 2002;33:369–74. doi:10.1016/S1359-835X(01)00116-6.

[23] Gowda TM, Naidu ACB, Chhaya R. Some mechanical properties of untreated jute fabric-reinforced polyester composites. Compos Part A Appl Sci Manuf 1999;30:277–84. doi:10.1016/S1359-835X(98)00157-2.

[24] Shah DU, Schubel PJ, Clifford MJ, Licence P. Fatigue life evaluation of aligned plant fibre composites through S-N curves and constant-life diagrams. Compos Sci Technol 2013;74:139–49. doi:10.1016/j.compscitech.2012.10.015.

[25] Rosa IM De, Santulli C, Sarasini F. Mechanical Characterization of Untreated Waste Office Paper/Woven Jute Fabric Hybrid Reinforced Epoxy Composites. J ofAppliedPolymer Sci 2011;119:1366–73. doi:10.1002/app.

[26] Quaresimin M. Multiaxial Fatigue Testing of Composites : From the Pioneers to Future Directions. Strain 2015;51:16–29. doi:10.1111/str.12124.

[27] Quaresimin M, Susmel L, Talreja R. Fatigue behaviour and life assessment of composite laminates under multiaxial loadings. Int J Fatigue 2010;32:2–16. doi:10.1016/j.ijfatigue.2009.02.012.

[28] Amijima S, Fujii T, Hamaguchi M. Static and fatigue tests of a woven glass fabric composite under biaxial tension-torsion loading. Composites 1991;22:281–9. doi:10.1016/0010-4361(91)90003-Y.

[29] Ogasawara T, Onta K, Yokozeki T, Ogihara S. Tension/Torsion Fatigue Behavior of Unidirectional GFRP and CFRP. Proc. 16th Int. Conf. Compos. Mater., 2007, p. 1–8.

[30] Sumsion HT, Rajapakse YDS. Simple torsion test for shear moduli determination of orthotropic composites 1978.

[31] Qi DT, Cheng GX. Fatiaue behavior of filament-wound glass fiber reinforced epoxy composite tension/torsion biaxial tubes under loading. Polym Compos 2007;28:116–23. doi:Doi 10.1002/Pc.20275.

[32] Curtis PT. The fatigue behaviour of fibrous composite materials. J Strain Anal Eng Des 1989;24:235–44.

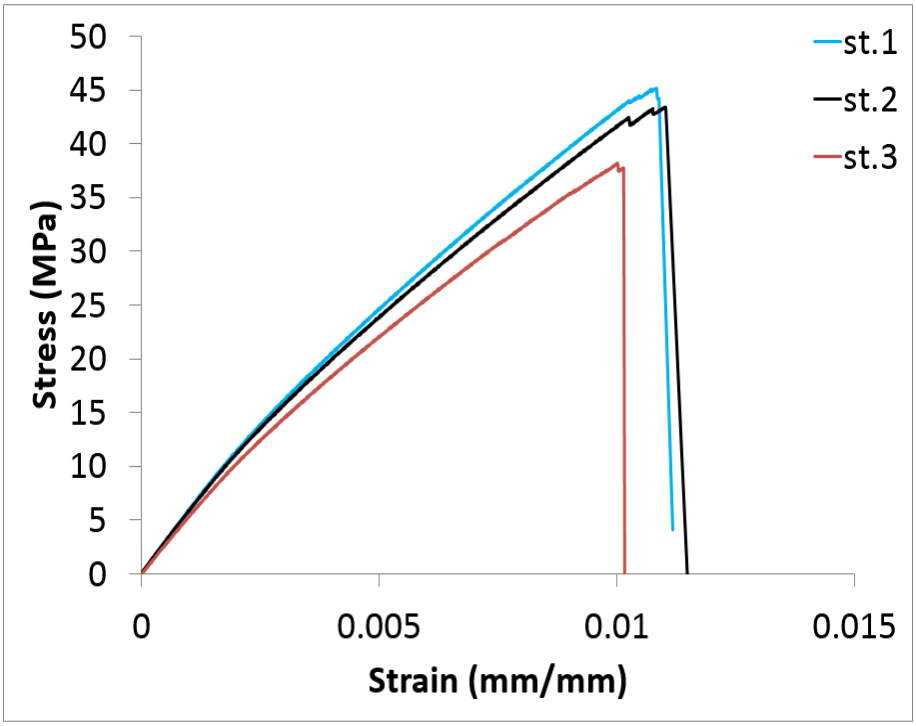

Fig.1 Stress-strain curves of the tensile static tests

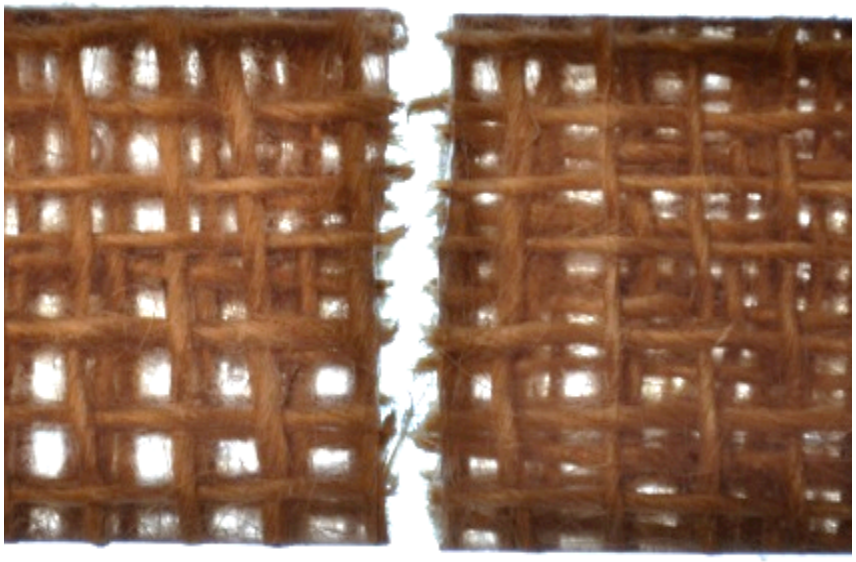

Fig.2 A JFRP sample post tensile static test

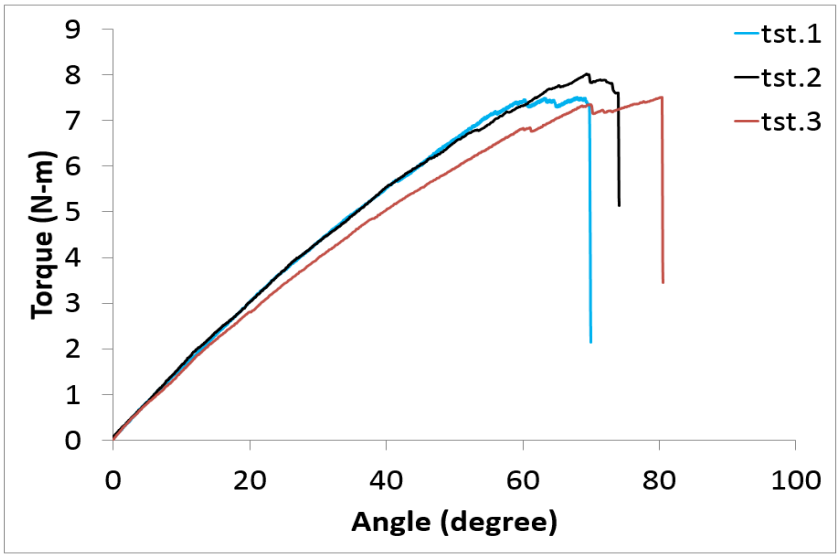

Fig.3 Torsional static torque versus angular displacement

Fig.4 Example of a JFRP sample post torsional static test

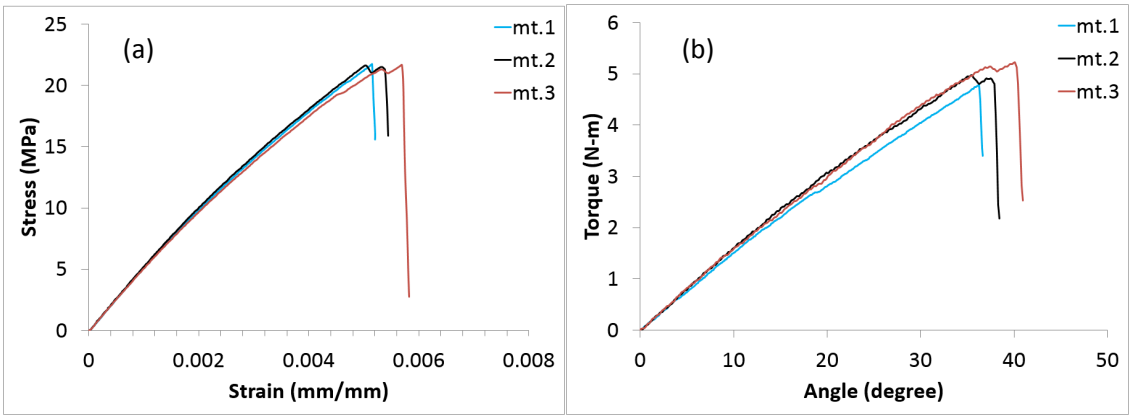

Fig.5 Multi-axial static test (a) stress vs strain (b) torque vs angle

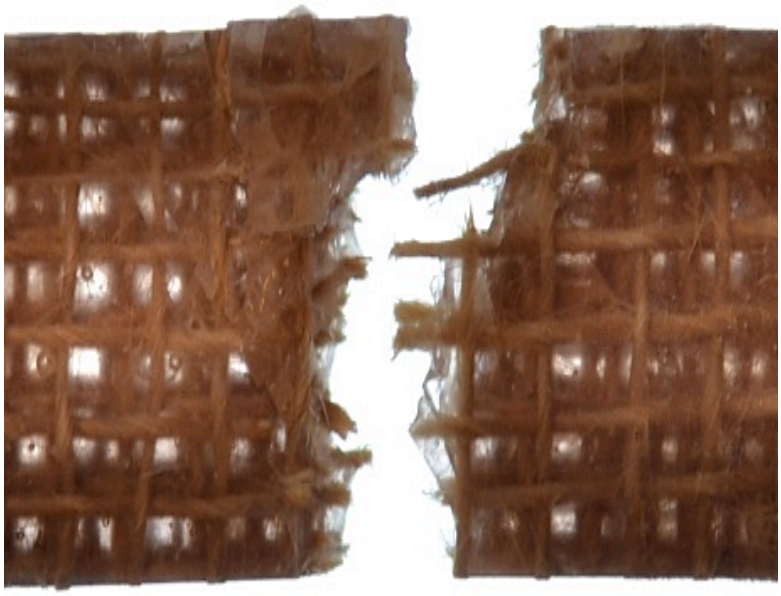

Fig.6 Fracture of a JFRP specimen after the multi-axial static test

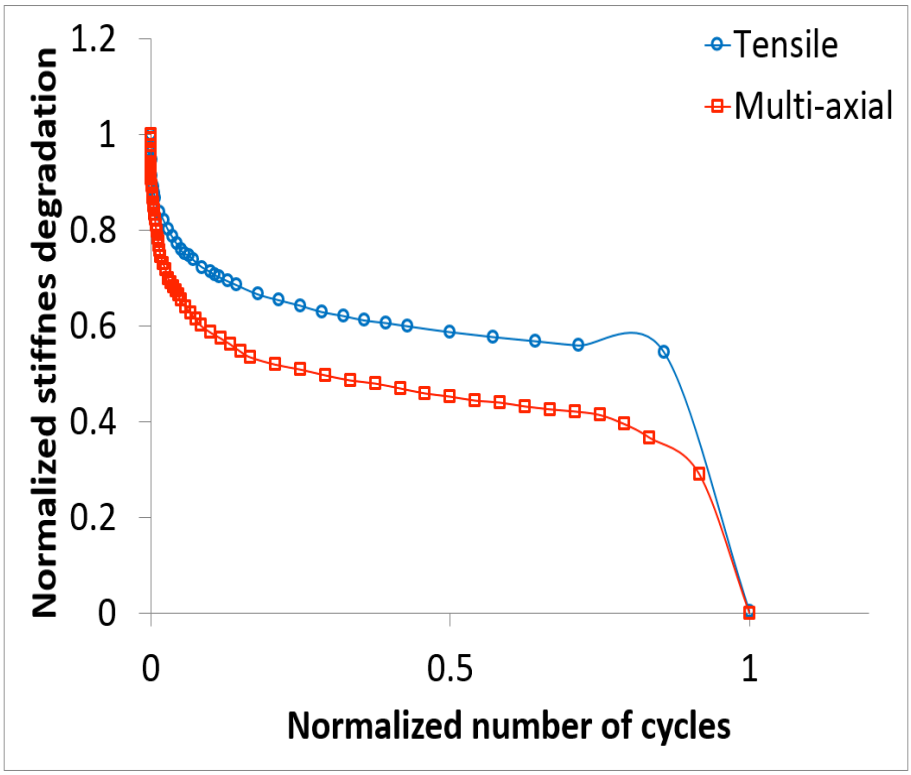

Fig.7 Normalized stiffness degradation

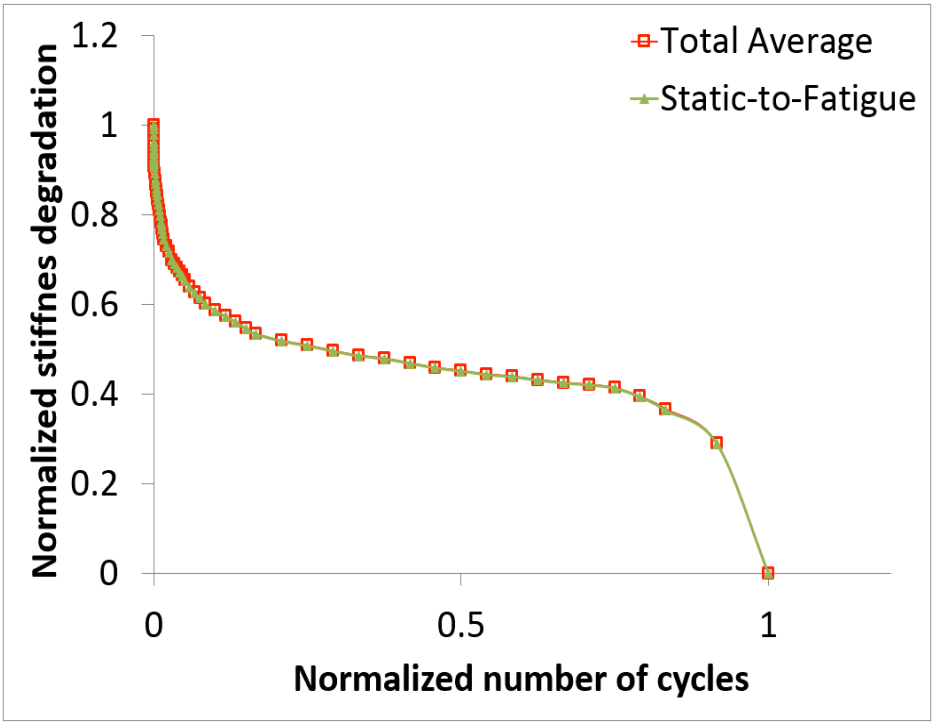

Fig.8 Multi-axial normalized stiffness degradation

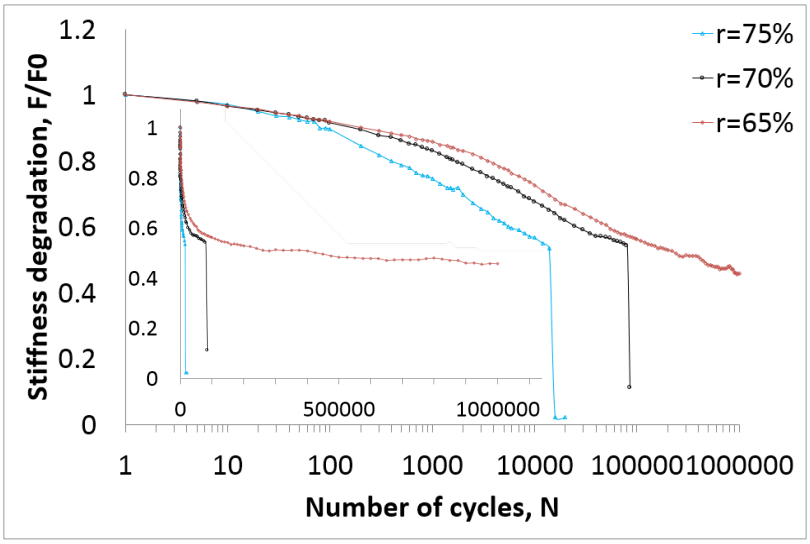

Fig.9 Stiffness degradation of tensile fatigue tests.

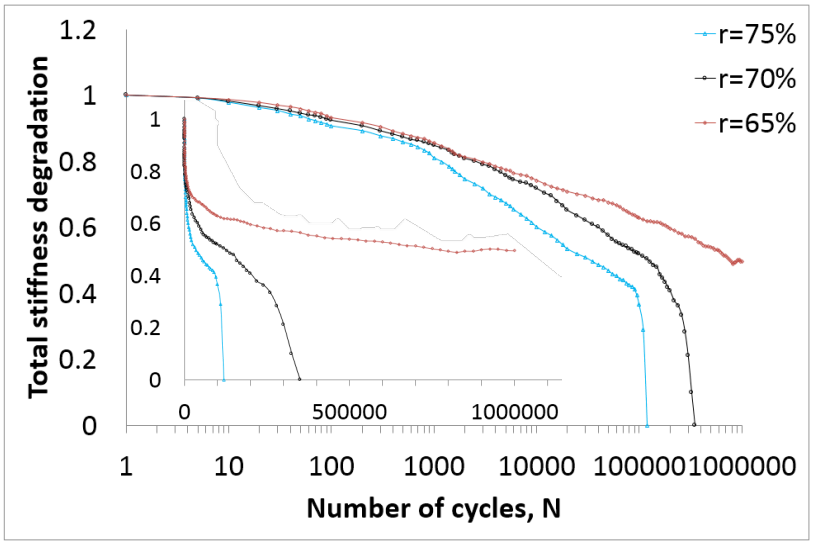

Fig.10 Stiffness degradation of multi-axial fatigue tests.

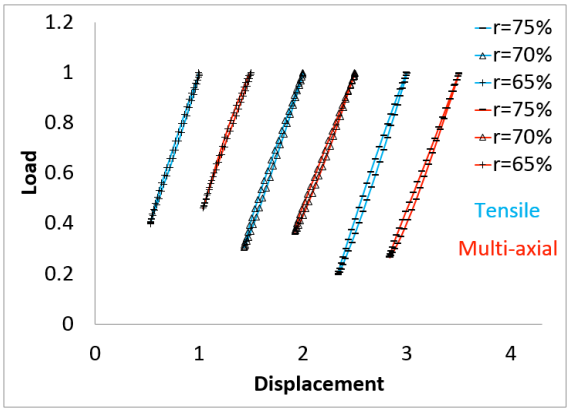

Fig.11 Comparison between hysteresis loops at $N = 1$ for different straining levels.

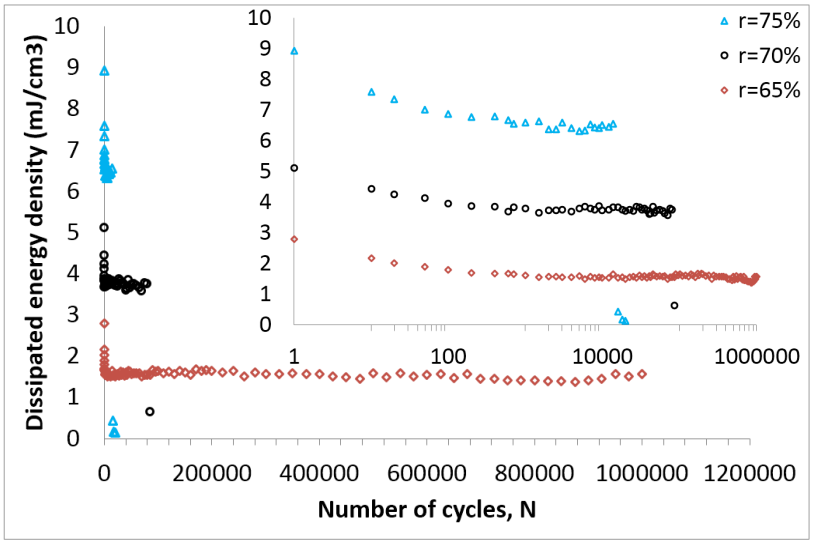

Fig.12 Dissipated energy density of tensile fatigue tests

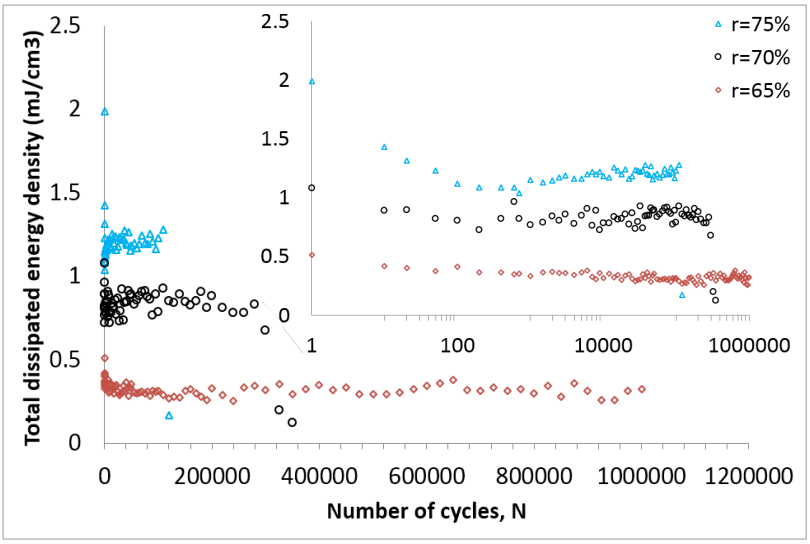

Fig.13 Total dissipated energy density of multi-axial fatigue tests

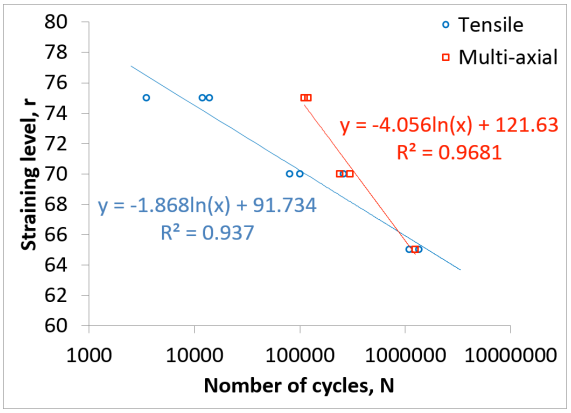

Fig.14 r-N curves for the tensile and multi-axial fatigue tests